# METHANOL SYNTHESIS IN A COUNTERCURRENT GAS–SOLID–SOLID TRICKLE FLOW REACTOR. AN EXPERIMENTAL STUDY

M. KUCZYNSKI, M. H. OYEVAAR, R. T. PIETERS and K. R. WESTERTERP[†]

Chemical Reaction Engineering Laboratories, Department of Chemical Engineering, Twente University of Technology, P.O. Box 217, 7500 AE Enschede, The Netherlands

**Abstract**—The synthesis of methanol from CO and $H_2$ was executed in a gas–solid–solid trickle flow reactor. The reactor consisted of three tubular reactor sections with cooling sections in between. The catalyst was Cu on alumina, the adsorbent was a silica–alumina powder and the experimental range 498–523 K, 5.0–6.3 MPa and 0.2–0.33 molar fraction of CO. Complete conversion in one pass was achieved for stoichiometric feed rates, so that the gas outlet could be closed. The experimental results are compared with the model presented in the previous paper [Westerterp, K. R. and Kuczynski, M. (1987) *Chem. Engng Sci.* 42,]; agreement is close over the entire conversion range from 15 % to 100 %.

## 1. INTRODUCTION

The methanol synthesis from carbon monoxide and hydrogen according to the following reaction:

$$CO + 2H_2 = CH_3OH, \quad -\Delta H(298\,K) = 91\,kJ\,mol^{-1} \tag{1}$$
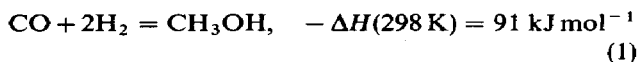
is one of the most important processes in the chemical industry. It also represents a wide category of processes based on heterogeneously catalysed equilibrium gas reactions. In such processes, owing to thermodynamic limitations, only certain per-pass reactant conversions can be attained in the reactor units. To obtain a reasonable degree of reactant utilization in such a reactor unit it is common practice to introduce product separators and reactant recycle loops. This is a cumbersome and expensive technique (Westerterp and Kuczynski, 1986). In our laboratories a research programme has been started dealing with new processes based on gaseous equilibrium reactions in which high reactant conversions can be attained, so that the expensive reactant recycling can be reduced or even suppressed. The economical significance of such a process improvement is discussed elsewhere (Westerterp and Kuczynski, 1986).

In this paper we report on our experimental study of the methanol synthesis in a countercurrent gas–solid–solid trickle flow reactor (GSSTFR). The principle of the GSSTFR is described in Westerterp and Kuczynski (1987). In fact, it is an extension of the gas–solid trickle flow (GSTF) principle, which has been investigated systematically by van Swaaij and co-workers (Roes, 1978; Roes and van Swaaij, 1979a–c; Verver, 1984; Noordergraaf *et al.*, 1980a–c). The most important aim of our study is to evaluate the technical feasibility of the GSSTFR for low-pressure methanol

synthesis and to draw more general conclusions concerning its applicability to other equilibrium processes. The following aspects are of particular interest:

(a) to examine whether complete conversion of the reactants can be achieved in a single-pass operation;

(b) to study the influence of various process parameters on the behaviour of the reactor; and

(c) to compare the experimental results obtained with the predictions of the mathematical reactor model presented in Westerterp and Kuczynski (1987).

## 2. EQUIPMENT AND CHEMICAL SYSTEM

### 2.1. *The experimental system*

A small-scale reactor system was constructed for experimental purposes. It consisted of three tubular packed-bed reactor sections in series and with intermediate cooling, a continuously operable gas feed system, a semicontinuously operable solids feed system and an on-line gas chromatographic analytical system. The process flow scheme is given in Fig. 1. All parts were made of 325M stainless steel.

### 2.2. *The reactor*

The reactor consisted of three vertical sections in series, 0.6, 0.6 and 0.55 m long (the upper being the shortest), having an inner diameter of $25 \times 10^{-3}$ m and an outer diameter of $60 \times 10^{-3}$ m. To facilitate removal of a possible excess of heat, cooling sections as shown in Fig. 2 were installed between the reactor sections. Water or air could be used as the cooling medium in these cooling sections. The synthesis gas was fed into the lower end of the lower reactor section and the product gas was removed at the top of the upper section. Support grids to support the catalyst packing in the reactor tubes were installed at the top of the cooling sections, as can be seen in Fig. 2. For the lower reactor section, the support grid was placed at

---

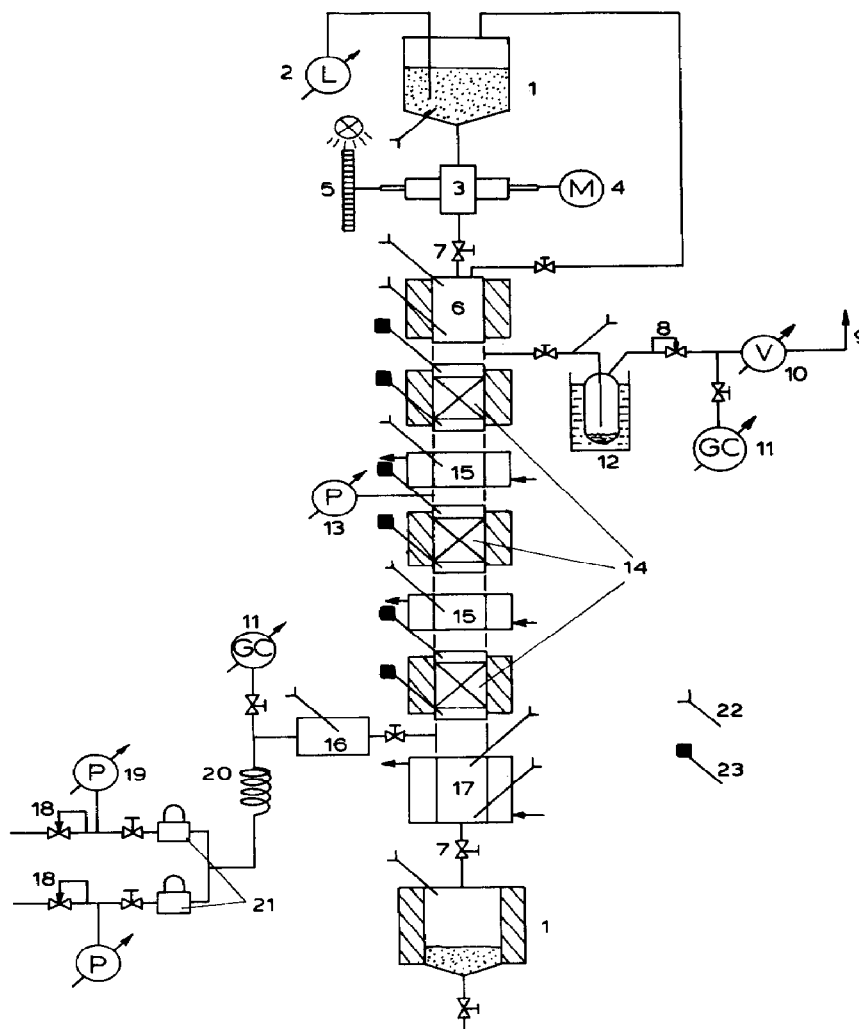[†] Author to whom correspondence should be addressed.

Fig. 1. The experimental gas–solid–solid trickle flow reactor. (1) Solids storage vessels; (2) solids level indicator; (3) solids feeder; (4) d.c. motor; (5) photo-electric revolution counter; (6) solids preheater; (7) ball valve; (8) back pressure regulator; (9) gas outlet; (10) wet gas flow meter; (11) sampling points; (12) cold trap unit; (13) electronic pressure transducer; (14) reactor sections; (15) cooling sections; (16) gas preheater; (17) solids cooler; (18) pressure regulators; (19) Bourdon-type manometers; (20) mixing pipe; (21) electronic mass flow controllers; (22) single thermocouple; (23) two thermocouples: one with the weld located in the reactor axis and the other one in the tube wall.

the top of the solids cooler installed below this section.

Commercial BASF copper catalyst type S3-85 was used. As active component it contains 30 wt % copper on an alumina carrier. The S3-85 catalyst is a modern, highly active methanol catalyst for the low-pressure process. It is very sensitive to poisoning by sulphur and phosphor compounds, requiring therefore synthesis gas of a high purity. The catalyst particles used in our experiments are $5 \times 5$ mm cylindrical pellets. To increase the void fraction of the bed we "diluted" the catalyst by adding $7 \times 7 \times 1$ glass Raschig rings to obtain a ratio of pellets to rings of $2:1$ by number. Each reactor section contained 91 g of catalyst.

### 2.3. The gas feed system

Previously prepared gas mixtures could be used or separate reactant gas streams could be mixed and fed into the reactor. In the latter case, the feed gas composition could be easily adjusted. Carbon monoxide was drawn from a battery of high-pressure storage cylinders, while for the hydrogen supply the high-pressure gas network of our high-pressure laboratory was used.

After pressure reduction by two Tescom Type 2600 pressure regulators, the reactant feed streams passed through electronic Brooks type 5850 TR mass flow meters/controllers. Prior to entering the reactor, the reactants were mixed in a helical mixing pipe and led through an electric gas preheater. A system of valves and connections was installed to check the calibration lines of the gas flow controllers with a wet gas meter as frequently as necessary, e.g. once a day.

Most experiments were carried out with a near stoichiometric $CO + H_2$ mixture. Several experiments
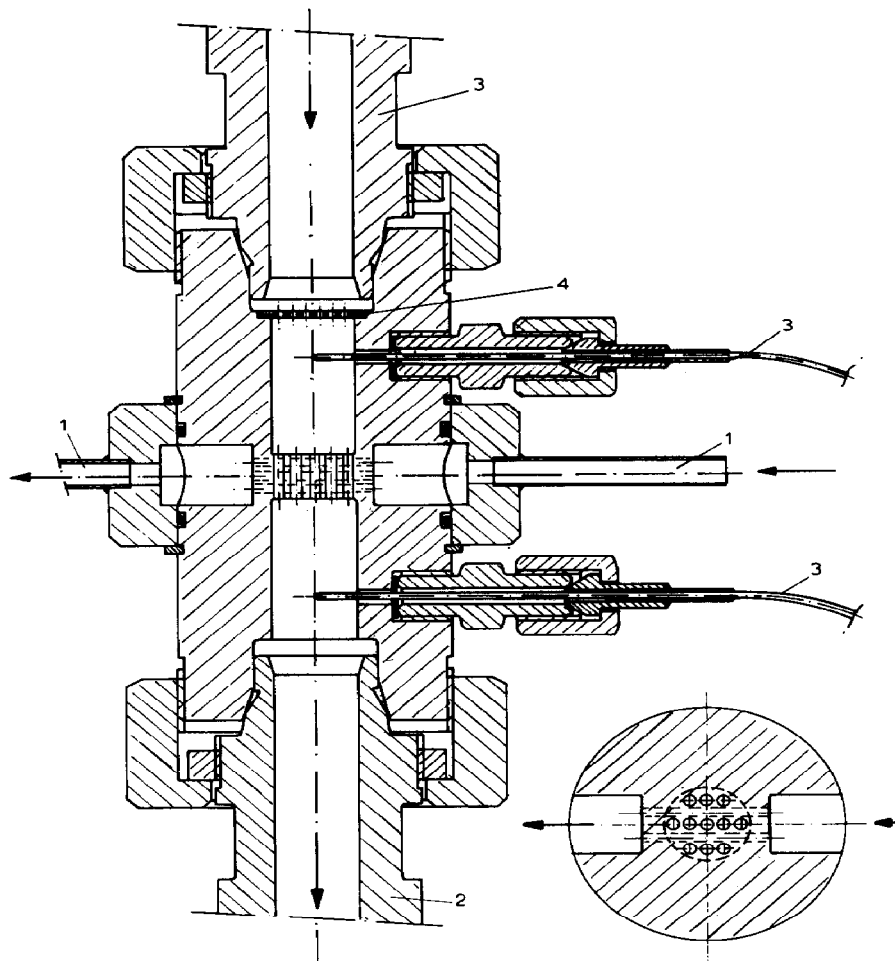
Fig. 2. Construction details of the cooling section line. The connections and flanges to the reactor sections are also shown. (1) Cooling medium ports; (2) reactor tubes; (3) thermocouples; (4) catalyst support grid.

were also done with an excess of hydrogen. The feed gas was free of carbon dioxide. The manufacturer's specifications (Hoek Loos) of the reactant gases are given in Table 1.

### 2.4. *The gas outlet*

The product gas left the reactor at the top of the upper reactor section. A Tescom model 1700 back pressure controller was installed at the gas outlet to control the total pressure in the reactor. A cold-trap vessel with a volume of $150 \times 10^{-6}$ m³ was installed just before the pressure controller to remove condensable components from the gaseous reactor ef-

fluent to prevent their condensing in the piping downstream. The rate of condensation could be determined by weighing the condensate accumulated during a known period of time. The dry effluent gas flow was measured by means of a wet-gas meter. Special care was taken to prevent condensation of methanol in the reactor in cold spots by installing additional electric heaters.

### 2.5. *The solids feed system*

The reactor was equipped with two storage vessels for the adsorbent supply and receival, respectively; the large capacity of these vessels enabled us to execute

Table 1. Volumetric composition of the feed gases. Manufacturer's specifications

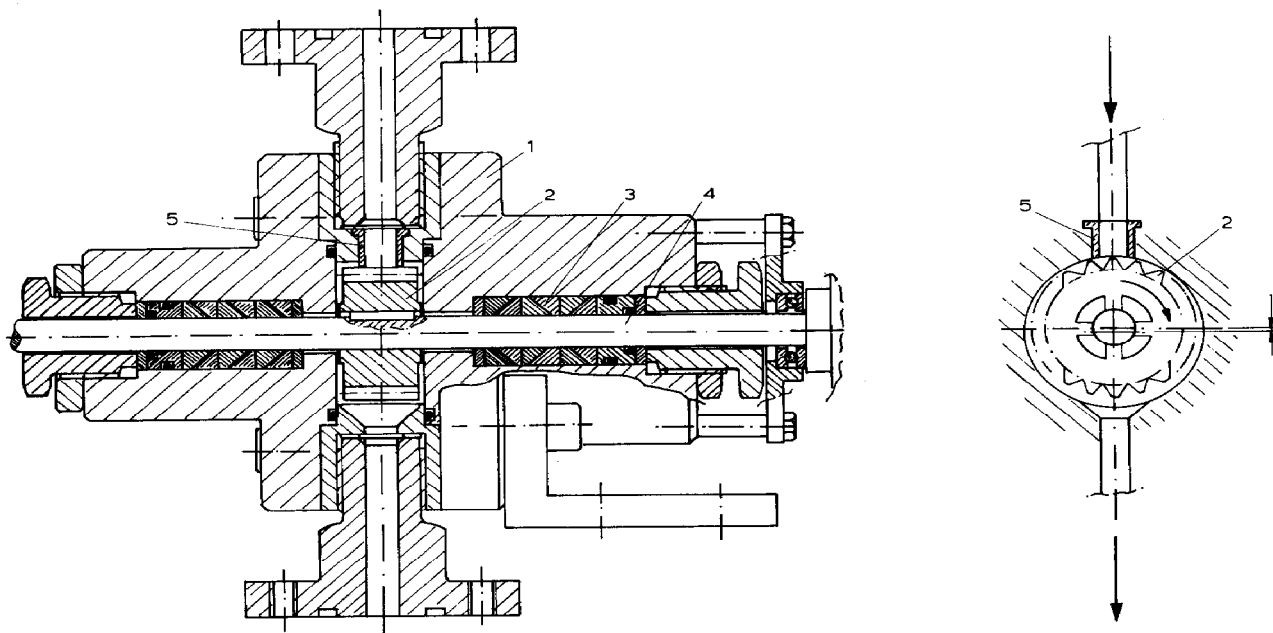| Component gas | CO | $H_2$ | $O_2$ | $N_2$ | $CO_2$ | Ar | Hydro-carbons | $H_2O$ |
|---|---|---|---|---|---|---|---|---|
| CO | > 99.5% | < 0.1% | — | < 0.3% | — | < 0.3% | <200 ppm | — |
| $H_2$ | < 5 ppm | > 99.9% | < 5 ppm | < 5 ppm | < 5 ppm | — | — | < 300 ppm |

Fig. 3. The solids feeder. (1) Housing; (2) Teflon rotor; (3) packing; (4) axle; (5) tubular Teflon socket.

experiments of a long duration without operating a cumbersome high-pressure solids recycling system. The storage vessels could contain 10 kg of the solid and enabled us to maintain a constant flow of solids for 4–20 h, depending on the operating conditions chosen. The upper vessel was equipped with an Endress & Hauser electronic level meter. The powder was continuously fed into the reactor by a special solids feeder (Fig. 3). The solids feeder was calibrated prior to the experiments.

To heat the solids stream entering the reactor up to the reaction temperature, a solids preheater was installed between the solids feeder and the upper reactor section. The construction of this preheater is outlined in Fig. 4. It consisted of a 0.5 m long vertical tube having the same outer and inner diameters as the reactor tubes. This tube was externally heated by an electric oven. To ensure good contact between the powder moving by gravity and the heated tube wall, a cylindrical bar was installed in the tube axis so that the solid fell through an annular channel. Between the lower reactor section and the lower storage vessel, a solids cooler of similar construction was installed. It was surrounded by a cooling water jacket.

Amorphous LA-25 low-alumina cracking catalyst (Akzo, Amsterdam) was used as the methanol adsorbent. Its physical properties are given in Table 2. The adsorption properties for methanol of LA-25 are described in Kuczynski *et al.* (1986b).

### 2.6. *The temperature and pressure recording and control*

Calibrated type K thermocouples and a Philips type PM 8237A multipoint data recorder were used for the temperature measurements. The thermocouples were
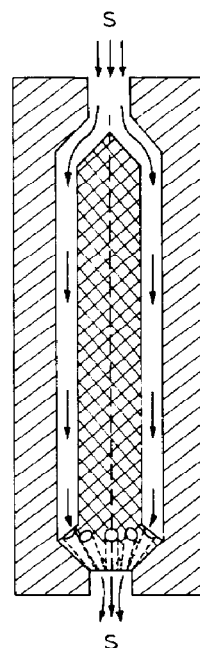


Fig. 4. The solids preheater and cooler. The solids stream passes through an externally heated or cooled annular channel.

installed under and above each catalyst bed (see Fig. 2) as well as at the outer wall of each reactor section. The reactor sections and the gas and solids preheaters were equipped with electric heating ovens, which were connected to Type 810 electronic temperature regulators (manufactured by Eurotherm). Several electronic pressure transducers of Bell & Howell as well as

Table 2. Properties of the methanol adsorbent

Composition: 87 wt % $SiO_2$, 13 wt % $Al_2O_3$.
Mean particle diameter: $ca.\ 90 \times 10^{-6}$ m
Skeletal density: 2200 $kg\,m^{-3}$
Particle density: 813 $kg\,m^{-3}$

Particle diameter distribution

| Diameter ($\mu$m) | Wt % | Cum. wt % |
|---|---|---|
| < 38 | 0.1 | 0.1 |
| 38–45 | 0.3 | 0.4 |
| 45–63 | 6.3 | 6.7 |
| 63–90 | 39.4 | 46.1 |
| 90–125 | 41.3 | 87.4 |
| 125–150 | 12.3 | 99.7 |
| > 150 | 0.3 | 100.0 |

Bourdon type gauges of Econosto were installed for pressure measurements, as shown in Fig. 1.

## 2.7. Gas analysis

A Varian series 3770 gas chromatograph with a thermal conductivity detector and an automatic sampling valve were used for the analysis of the feed and product gases. The sampling valve was coupled to a Hewlett–Packard 3390A integrator and a Hewlett–Packard 19400A sample/event unit, so that on-line operation was possible. Hydrogen was used as carrier gas. The gas streams could be sampled continuously by means of an automatically controlled Watson–Marlow peristaltic pump, either at the bottom or at the top of the reactor. A 1/8″ diameter and 1.5 m long Porapak-Q column was used for the analysis. The detector was found to be linear for carbon monoxide, methanol, water and dimethyl ether in the concentration ranges of interest. The calibration lines were checked prior to each experimental run, using calibrated gas mixtures.

The chemicals used for the calibration of the GC were of the following qualities: CO and $H_2$ as specified in Table 1, methanol > 99.95 % (from Merck), dimethyl ether > 99 vol. % (from Hoek Loos).

## 2.8. Initial testing, calibration and start-up

The individual pieces of equipment were tested for leaks using hydrogen at a pressure of 12 MPa. The solids feeder, the solids level meter and the pressure gauges were then tested and calibrated.

## 2.9. Catalyst activation

The catalyst was reduced according to the manufacturer's instructions. The reactor was filled with catalyst and then first rinsed with nitrogen containing 2 vol. % hydrogen and heated slowly up to 453 K in a period of 3 h. Subsequently the heating up was continued at a rate of 5 $K\,h^{-1}$, up to 513 K. At the same time, the $H_2$ content in the feed gas was gradually increased up to 20 vol. % at 513 K. The rinsing was then continued until water was no longer detected in the reactor effluent. After the catalyst reduction the feed was switched to a synthesis gas containing 20 vol. % CO and 80 vol. % $H_2$; with this feed, the reactor was kept at 513 K and 6 MPa for 72 h to enable the catalyst to attain a stable activity level. This was followed by frequent analysis of the reaction product. The catalyst was considered to be stable if under stable operating conditions in a period of 24 h the conversion did not change.

## 2.10. Experimental difficulties during start-up

The majority of the mechanical problems encountered related to the solids feeder, in particular clogging with powder and damage to the rotor. After numerous changes, the final solution was obtained with a rotor made of Teflon installed eccentrically in a cylindrical chamber, as shown in Fig. 3. Also the shape of the inlet channel to the rotor was found to be very important.

## 3. EXPERIMENTAL

### 3.1. Typical experiments

Two slightly different experimental procedures were followed depending on whether or not complete reactant conversion was desired. The preparation, the start-up procedure and the method of analysis of the solids were the same in both cases.

Prior to the filling of the upper storage tank with adsorbent, the installation was depressurized under rinsing with hydrogen. The powder was previously dried by keeping it for 48 h under vacuum at 553 K. After that the entire installation and specially the storage vessel was rinsed radically by pressurizing it with hydrogen up to a pressure of 1 MPa and then expanding it to atmospheric pressure again, repeating this procedure five times.

During the solids regeneration, care was taken to conduct the desorption procedure always under the same conditions (48 h at 553 K) and to minimize the time of exposure of the dried powder to the atmosphere during the filling. The same powder charge was used in all the experiments during a period of 12 months.

For quantitative evaluation of a possible catalyst degradation, CO conversion experiments were frequently carried out with the solids feed system turned off. In this way, data were also gathered allowing a direct evaluation of the influence of the solids stream on the reactor performance.

### 3.2. Experiments with an open gas outlet

To start an experiment, the required flows and composition of the feed gas were adjusted with the gas flow controllers, wheras the total pressure was set using the back pressure controller at the reactor outlet. After the gas flow and the gas composition at the reactor outlet became steady (1–4 h depending on the feed flow and the reactor temperature), the methanol production rate was determined. Then the adsorbent supply was started at the required flow. After a steady state was reached, the flow and composition of the product gas, as well as the methanol condensation rate in the cold-trap unit, were measured again. After the experiment, a

solids sample could be taken from the lower storage tank and analysed. During the experiments, both the lower and upper solids storage tanks were maintained at room temperature.

### 3.3. *Experiments with a closed gas outlet*

Before the experiment, the entire apparatus was first rinsed with hydrogen and then pressurized with a stoichiometric $CO/H_2$ mixture. After the solids feed was turned on, the pressure in the reactor started to decrease due to the methanol adsorption. Then the pressure was kept constant by feeding synthesis gas and the gas flow necessary to maintain the pressure was determined. Again the solids could be sampled from the lower storage tank.

### 3.4. *Checking the material balance by analysis of the solids*

To check the overall material balance, an analysis of the solids had to be made. To this end, a simple glass apparatus as shown in Fig. 5 was used. After a run with the GSSTFR, a solids sample was taken from the lower storage tank and introduced into a glass flask. During this sample taking, a small, unavoidable loss of $CH_3OH$ occurred. About 100 g of this solid was heated slowly up to 540 K and simultaneously the gas above the solid was evacuated and passed through a cold trap, which was placed in a liquid nitrogen bath. Afterwards the condensate was weighed and analysed. The solids analysis was not performed after each experimental run because each time the reactor was opened a cumbersome and costly rinsing and leak test procedure had to be followed. Therefore, the solids analysis was done only once after every eight experiments in order to check the overall mass balance and to examine the composition of the adsorbate.

### 3.5. *Corrections to the temperature readouts*

As shown in Fig. 2, the thermocouples were installed perpendicular to the reactor wall in such a way that their welds were located exactly in the reactor axis. The temperature readings are distorted by the heat conductance of the thermocouple tube, so that the reading will be in between the wall temprature and the real gas temperature. The wall temperature will be uniform in the axial direction due to the large wall thickness. Assuming that the temperature and the linear velocity of the gas are uniform over the whole reactor cross-section, the true gas temperature can be
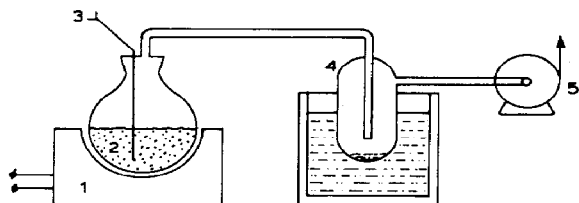


Fig. 5. Apparatus for the analysis of the solids. (1) Heating oven; (2) solids sample; (3) thermocouple; (4) cold trap; (5) vacuum pump.

calculated based on the experimental data (see the Appendix).

### 3.6. *The catalyst activity*

The decrease of the catalyst activity was linear with time: 6 months after start-up the catalyst activity was 30 % lower than its initial activity. We ascribe this effect possibly to the absence of carbon dioxide in the gas phase (Kuczynski *et al.*, 1986a) and for sure to rough handling of the catalyst: our reactor was started up and shut down three times a week on the average. An effect of the adsorbent stream on the catalyst performance cannot be excluded either: small particles of crushed adsorbent may, for example, block the macropores of the catalyst, leading to a decrease of its active surface area.

In the course of the initial and start-up experiments, we observed that a total loss of catalyst activity occurred very quickly, e.g. within 48 h, in cases where the reactor had not been rinsed with hydrogen or an inert gas in between the experimental runs. This deactivation was irreversible. Possibly a consecutive product from a slow decomposition of methanol has a destructive influence on the catalyst. To avoid this effect, we thereafter kept the catalyst beds always in a hydrogen atmosphere in the periods between experiments.

### 3.7. *Accuracy of the experiments*

The estimated accuracy of the calibrated thermocouples used was about 0.25 K and the error in the pressure measurements was less than 0.025 MPa. The accuracy of the calibration line of the solids feeder lay within 4 % of the value measured, whereas that of the wet-gas meters was better than 0.5 %. The estimated maximum error of the GC analysis amounted to 0.3 vol. % for each component. There were several additional sources of scatter in the experimental data. We believe the catalyst promotion by side products to be the most important one.

### 3.8. *Influence of oxygen and water on the catalyst*

As has already been mentioned, during the filling of the upper solids storage tank, the adsorbent was exposed for a short time to the open air, so that adsorption of oxygen and water could not be avoided. According to recent research on the kinetics of methanol synthesis (see, for example, Herman *et al.*, 1979), even small amounts of water and oxygen can influence the methanol formation rate strongly. Therefore the system was radically rinsed with hydrogen after filling the solids storage vessel and prior to the experiments. Nevertheless, remaining traces of $O_2$ or $H_2O$ may have promoted the catalyst activity.

### 3.9. *CO and $H_2$ co-adsorption*

The powder contained in the upper storage tank is free from methanol whereas the adsorbent collected in the lower vessel contains methanol. Although the temperatures of both tanks were maintained at the same level, the adsorption properties of the powder for

Table 3. Experimental data for a closed reactor outlet

| Expt No. | $\bar{T}$ (K) | $p$ (MPa) | $E$ | $R_p \times 10^3$ (mol MeOH (kg cat s)$^{-1}$ as measured) | $\phi_s \times 10^3$ (kg s$^{-1}$ experimental) |
|---|---|---|---|---|---|
| 1 | 498 | 5.16 | 22.6 | 0.47 | 0.20 |
| 2 | 499.9 | 5.94 | 17.3 | 0.71 | 0.20 |
| 3 | 501 | 6.01 | 35 | 0.59 | 0.34 |
| 4 | 509.1 | 6.21 | 21 | 1.05 | 0.35 |
| 5 | 512.2 | 6.21 | 15.5 | 1.42 | 0.35 |
| 6 | 512.5 | 5.90 | 27 | 1.10 | 0.50 |
| 7 | 513 | 5.10 | 12.3 | 0.86 | 0.20 |
| 8 | 513 | 5.10 | 20.7 | 1.07 | 0.43 |
| 9 | 513 | 6.74 | 21.9 | 1.55 | 0.50 |
| 10 | 513.1 | 5.01 | 25.6 | 0.98 | 0.49 |
| 11 | 523.3 | 5.10 | 18 | 1.23 | 0.43 |
| 12 | 524 | 5.00 | 19.2 | 1.31 | 0.50 |

CO and $H_2$ may depend on the methanol concentration. To evaluate possible errors in the calculated CO conversions caused by the co-adsorption of carbon monoxide, several simple adsorption tests based on the total pressure measurements were carried out at 492–523 K and under a total pressure of 6 MPa. We found that the CO adsorption had no significant implication on our experimenal accuracy.

## 4. RESULTS AND DISCUSSION

In total 12 experiments with a closed and 90 experiments with an open gas outlet were carried out. In Table 3 the experimental data with a closed gas outlet are specified. Since in these experiments the mole fraction $y_{CO,in}$ of CO in the feed gas was always one-third and the total mass $m_{cat}$ of the catalyst was always 273 g, the molar flow of the feed gas can be easily calculated based on the reaction rate specified in Table 3 from

$$\phi_{in} = \frac{R_p m_{cat}}{y_{CO,in}}. \qquad (2)$$

$E$ represents the adsorption number, defined by (Westerterp and Kuczynski, 1987)

$$E = \frac{\phi_s m(T_R) p}{\rho_s \phi_{in} y_{CO,in} R T_R} \qquad (3)$$

where $T_R$ is a reference temperature. This adsorption number expresses the ratio of the flow rate of the adsorbent to the feed flow rate of the gas. $m(T_R)$ is the distribution factor for the adsorption of methanol and is expressed by (Westerterp and Kuczynski, 1987) $m = 0.145 \exp 2304/(T/K)$. As there was no gas bled off, the reactant conversion was complete. The reactor capacity is calculated on the basis of the determined gas feed flow. The results with an open reactor outlet are listed in Table 4. The conversion of CO in these experiments is calculated on the basis of the molar flows of CO measured at the reactor inlet and outlet:

$$\zeta_{CO} = \frac{\phi_{CO,in} - \phi_{CO,out}}{\phi_{CO,in}}. \qquad (4)$$

$\delta$ in Table 4 is the catalyst activity factor expressing the

ratio of the reaction rates measured in standard experiments to those measured under identical conditions for the fresh catalyst. It is thus a direct measure of the residual activity of the catalyst since start-up. To correct for the catalyst activity in comparing the model (Westerterp and Kuczynski, 1987) with the experiments, now the Damköhler number $Da$ can be reduced to $\delta Da$, which is equivalent to reducing the methanol production rate $R_p$ to $\delta R_p$.

$\alpha^*$ is the distribution factor of the methanol produced and equals the ratio of the carry-over of methanol in the gaseous reactor effluent to the total production rate of methanol. From an analysis of the solids in the receival vessel the adsorbate was found to consist almost exclusively of methanol, the remainder being water and dimethyl ether. The reactor capacity appears to increase with an increase of the total pressure, the temperature or the solids flow. Such an influence of the pressure and temperature results from the reaction kinetics (Kuczynski et al., 1986a), whereas the solids flow determines the methanol partial pressure in the reactor influencing in this way the reaction rate, as discussed in our previous paper (Westerterp and Kuczynski, 1987). For high solids flow rates, the reaction rate approaches the initial reaction rate because the methanol partial pressure is kept low and the reverse reaction does not take place. On the other hand, however, the methanol concentration in the solid phase decreases.

The behaviour of the GSSTFR and the influence of the most important operating and design variables on its performance have been amply discussed in the previous paper, in which a mathematical description of this type of reactor was given. The question still remains whether the mathematical description presented (Westerterp and Kuczynski, 1987) is confirmed by the experimental evidence. To this end, we will compare our experimental data with the predictions by the model. The question arises as to what are, in our experiments, the true temperatures at which the reaction takes place. For heterogeneously catalysed gas reactions this is the temperature of the catalyst, which in our experimental system cannot be measured di-

Table 4. Experimental data for an open reactor outlet

| Expt No. | $\bar{T}$ (K) | $p$ (MPa) | $y_{CO,in}$ | $E$ | $\phi_{in} \times 10^3$ (mol s$^{-1}$) | $\zeta_{CO}$ | $\delta$ | $\alpha^*$ |
|---|---|---|---|---|---|---|---|---|
| | | | Stoichiometric reactant mixture | | | | | |
| 1 | 497.8 | 6.05 | 0.326 | 7.6 | 1.5 | 0.377 | 1.00 | 0.010 |
| 2 | 498.2 | 6.31 | 0.330 | 4.7 | 2.3 | 0.278 | 1.00 | 0.020 |
| 3[†] | 498.3 | 6.05 | 0.340 | 9.6 | 1.5 | 0.424 | 0.91 | 0.010 |
| 4 | 498.3 | 6.17 | 0.330 | 5.2 | 2.3 | 0.213 | 1.00 | 0.003 |
| 5 | 498.3 | 6.22 | 0.330 | 6.7 | 2.2 | 0.229 | 1.00 | 0.004 |
| 6 | 498.3 | 6.26 | 0.330 | 4.8 | 2.2 | 0.200 | 0.95 | 0.011 |
| 7 | 498.4 | 6.29 | 0.330 | 6.6 | 2.3 | 0.290 | 1.00 | 0.048 |
| 8 | 498.5 | 6.13 | 0.334 | 6.2 | 1.9 | 0.275 | 1.00 | 0.027 |
| 9 | 498.5 | 6.15 | 0.315 | 5.7 | 1.9 | 0.340 | 1.00 | 0.016 |
| 10 | 498.6 | 6.16 | 0.334 | 3.2 | 1.9 | 0.309 | 1.00 | 0.049 |
| 11 | 498.7 | 6.06 | 0.317 | 4.2 | 1.5 | 0.419 | 1.00 | 0.029 |
| 12 | 498.7 | 6.18 | 0.335 | 2.7 | 2.3 | 0.270 | 1.00 | 0.076 |
| 13 | 498.8 | 6.07 | 0.330 | 10.0 | 1.5 | 0.394 | 1.00 | 0.005 |
| 14 | 498.9 | 6.14 | 0.315 | 8.1 | 1.9 | 0.303 | 1.00 | 0.018 |
| 15 | 499.2 | 6.30 | 0.339 | 4.1 | 2.5 | 0.187 | 1.00 | 0.070 |
| 16 | 499.2 | 6.31 | 0.332 | 2.2 | 2.9 | 0.225 | 1.00 | 0.106 |
| 17 | 499.3 | 6.07 | 0.317 | 7.2 | 1.5 | 0.433 | 1.00 | 0.005 |
| 18 | 500.2 | 6.19 | 0.330 | 5.2 | 2.3 | 0.307 | 1.00 | 0.026 |
| 19 | 500.2 | 6.30 | 0.334 | 5.4 | 2.8 | 0.239 | 1.00 | 0.032 |
| 20[†] | 501.3 | 6.32 | 0.338 | 3.6 | 2.9 | 0.277 | 0.91 | 0.032 |
| 21 | 501.5 | 6.06 | 0.330 | 4.1 | 1.5 | 0.401 | 1.00 | 0.037 |
| 22 | 501.8 | 6.32 | 0.338 | 5.1 | 2.9 | 0.222 | 1.00 | 0.012 |
| 23 | 502.0 | 6.06 | 0.325 | 6.9 | 1.5 | 0.414 | 1.00 | 0.011 |
| 24 | 502.1 | 6.04 | 0.340 | 7.6 | 1.5 | 0.457 | 1.00 | 0.001 |
| 25 | 502.8 | 6.26 | 0.334 | 4.2 | 2.8 | 0.147 | 0.70 | 0.027 |
| 26[†] | 503.4 | 6.29 | 0.332 | 4.2 | 2.9 | 0.297 | 0.91 | 0.018 |
| 27[†] | 508.3 | 6.22 | 0.347 | 2.6 | 2.2 | 0.652 | 0.91 | 0.048 |
| 28[†] | 508.7 | 6.18 | 0.331 | 3.3 | 1.9 | 0.711 | 0.91 | 0.017 |
| 29 | 508.9 | 6.23 | 0.337 | 4.1 | 2.9 | 0.267 | 1.00 | 0.283 |
| 30 | 509.2 | 6.18 | 0.315 | 6.7 | 1.9 | 0.642 | 1.00 | 0.020 |
| 31 | 509.3 | 6.02 | 0.334 | 4.9 | 2.9 | 0.267 | 1.00 | 0.062 |
| 32 | 509.3 | 6.27 | 0.331 | 3.7 | 2.9 | 0.357 | 1.00 | 0.126 |
| 33 | 509.4 | 6.01 | 0.330 | 6.4 | 2.3 | 0.296 | 0.70 | 0.056 |
| 34 | 509.4 | 6.09 | 0.319 | 8.1 | 1.9 | 0.363 | 0.70 | 0.045 |
| 35 | 510.0 | 6.24 | 0.331 | 2.2 | 2.9 | 0.301 | 1.00 | 0.257 |
| 36 | 510.1 | 6.18 | 0.335 | 7.9 | 1.9 | 0.503 | 1.00 | 0.014 |
| 37 | 510.6 | 6.19 | 0.335 | 6.3 | 1.9 | 0.511 | 1.00 | 0.008 |
| 38[†] | 511.3 | 6.26 | 0.332 | 5.2 | 2.9 | 0.479 | 0.91 | 0.022 |
| 39[†] | 511.9 | 6.17 | 0.330 | 10.4 | 1.4 | 0.825 | 0.91 | 0.014 |
| 40 | 512.0 | 6.25 | 0.347 | 6.5 | 2.2 | 0.478 | 1.00 | 0.023 |
| 41 | 512.1 | 6.29 | 0.351 | 4.4 | 2.3 | 0.498 | 1.00 | 0.010 |
| 42[†] | 512.4 | 6.23 | 0.344 | 5.5 | 1.9 | 0.634 | 0.91 | 0.014 |
| 43[†] | 513.9 | 6.15 | 0.351 | 7.0 | 1.6 | 0.833 | 0.91 | 0.018 |
| 44[†] | 514.2 | 6.15 | 0.345 | 3.7 | 1.6 | 0.884 | 0.95 | 0.200 |
| 45[†] | 515.2 | 6.16 | 0.333 | 6.7 | 1.6 | 0.911 | 1.00 | 0.010 |
| 46 | 518.6 | 6.11 | 0.316 | 8.0 | 1.9 | 0.507 | 0.70 | 0.019 |
| 47 | 518.7 | 6.13 | 0.318 | 5.7 | 1.9 | 0.547 | 0.80 | 0.036 |
| 48 | 518.8 | 6.06 | 0.318 | 6.4 | 1.9 | 0.438 | 0.70 | 0.024 |
| 49 | 519.0 | 6.07 | 0.322 | 6.2 | 1.7 | 0.429 | 0.70 | 0.033 |
| 50 | 519.1 | 6.07 | 0.322 | 3.6 | 1.7 | 0.510 | 0.72 | 0.077 |
| 51 | 519.1 | 6.16 | 0.320 | 7.9 | 1.5 | 0.659 | 0.70 | 0.010 |
| 52 | 519.6 | 6.06 | 0.320 | 4.4 | 1.4 | 0.664 | 0.70 | 0.039 |
| 53 | 519.8 | 6.15 | 0.320 | 10.0 | 1.5 | 0.619 | 0.70 | 0.012 |
| 54 | 519.9 | 6.18 | 0.330 | 5.3 | 2.2 | 0.510 | 0.90 | 0.063 |
| 55 | 520.0 | 6.07 | 0.317 | 8.0 | 1.5 | 0.680 | 0.63 | 0.089 |
| 56 | 520.0 | 6.39 | 0.346 | 2.0 | 3.0 | 0.353 | 1.00 | 0.168 |
| 57 | 520.1 | 6.14 | 0.329 | 2.7 | 2.3 | 0.473 | 1.00 | 0.239 |
| 58 | 520.7 | 6.06 | 0.317 | 7.1 | 1.5 | 0.705 | 0.70 | 0.032 |
| 59 | 520.8 | 6.27 | 0.345 | 3.9 | 3.01 | 0.417 | 1.00 | 0.113 |
| 60 | 521.0 | 6.40 | 0.346 | 3.4 | 3.04 | 0.380 | 1.00 | 0.078 |
| 61 | 522.3 | 6.24 | 0.330 | 6.8 | 2.24 | 0.509 | 1.00 | 0.032 |
| 62 | 523.6 | 6.16 | 0.328 | 2.1 | 2.94 | 0.298 | 1.00 | 0.232 |
| 63 | 523.7 | 5.99 | 0.316 | 3.3 | 1.88 | 0.484 | 0.63 | 0.173 |
| 64 | 523.7 | 6.03 | 0.325 | 2.7 | 2.27 | 0.492 | 1.00 | 0.156 |
| 65 | 524.1 | 5.92 | 0.316 | 3.3 | 1.87 | 0.578 | 0.80 | 0.152 |
| 66 | 524.1 | 6.03 | 0.327 | 4.6 | 2.25 | 0.520 | 0.80 | 0.069 |
| 67 | 524.2 | 6.17 | 0.328 | 3.6 | 2.94 | 0.341 | 0.67 | 0.139 |
| 68 | 524.4 | 6.03 | 0.327 | 5.2 | 2.25 | 0.513 | 1.00 | 0.060 |

*(Contd.)*

Table 4. (*Contd.*)

| Expt No. | $\bar{T}$ (K) | $p$ (MPa) | $y_{CO,in}$ | $E$ | $\phi_{in} \times 10^3$ (mol s$^{-1}$) | $\zeta_{CO}$ | $\delta$ | $\alpha^*$ |
|---|---|---|---|---|---|---|---|---|
| | | | Stoichiometric reactant mixture | | | | | |
| 69 | 524.4 | 6.15 | 0.328 | 4.1 | 2.94 | 0.343 | 0.70 | 0.124 |
| 70 | 524.7 | 5.96 | 0.321 | 4.0 | 1.54 | 0.713 | 0.70 | 0.117 |
| 71 | 524.7 | 5.98 | 0.316 | 8.1 | 1.88 | 0.572 | 0.70 | 0.040 |
| 72 | 524.8 | 5.93 | 0.321 | 6.4 | 1.85 | 0.591 | 0.75 | 0.053 |
| 73 | 524.8 | 6.04 | 0.327 | 6.6 | 2.25 | 0.507 | 0.70 | 0.001 |
| 74[†] | 524.9 | 6.14 | 0.329 | 4.7 | 2.27 | 0.677 | 0.83 | 0.084 |
| 75 | 525.0 | 6.21 | 0.321 | 5.1 | 3.06 | 0.421 | 0.70 | 0.082 |
| 76 | 525.1 | 5.97 | 0.316 | 5.7 | 1.87 | 0.570 | 0.90 | 0.072 |
| 77 | 525.6 | 6.02 | 0.314 | 7.8 | 1.56 | 0.637 | 0.70 | 0.013 |
| 78 | 525.8 | 6.01 | 0.314 | 9.8 | 1.56 | 0.681 | 0.70 | 0.018 |
| 79 | 526.0 | 6.30 | 0.336 | 5.1 | 2.97 | 0.456 | 0.90 | 0.109 |
| 80[†] | 528.5 | 5.97 | 0.321 | 6.8 | 1.54 | 0.724 | 0.91 | 0.032 |
| | | | Non-stoichiometric reactant mixture | | | | | |
| 81 | 500.0 | 6.04 | 0.200 | 10.9 | 0.89 | 0.867 | 0.95 | 0.089 |
| 82 | 500.3 | 6.05 | 0.200 | 5.1 | 1.11 | 0.711 | 0.70 | 0.055 |
| 83 | 507.7 | 6.24 | 0.250 | 6.8 | 1.34 | 0.900 | 0.90 | 0.017 |
| 84 | 508.0 | 6.23 | 0.250 | 6.3 | 1.44 | 0.844 | 0.80 | 0.021 |
| 85 | 508.2 | 6.23 | 0.250 | 4.8 | 1.90 | 0.642 | 1.00 | 0.062 |
| 86 | 510.0 | 5.05 | 0.200 | 5.3 | 1.52 | 0.678 | 0.70 | 0.010 |
| 87 | 510.0 | 6.05 | 0.250 | 4.7 | 1.65 | 0.820 | 0.90 | 0.030 |
| 88 | 512.2 | 6.21 | 0.250 | 5.9 | 1.90 | 0.840 | 0.90 | 0.015 |
| 89 | 514.2 | 6.04 | 0.210 | 4.3 | 2.16 | 0.690 | 0.70 | 0.030 |
| 90 | 523.2 | 6.04 | 0.210 | 4.7 | 2.78 | 0.727 | 0.80 | 0.021 |

[†]Mass of catalyst 110 g per reactor section.

rectly. The thermocouples are located below and above each catalyst bed and at the wall of each reactor section. In Table 5 typical results of the temperature measurements are given for the GSSTFR. In each reactor section the temperature of the gas appears to decrease slightly in the upward direction. In the case of no solids flow, the reverse effect—a slight increase in the temperature—was observed. The difference in the temperatures measured below and above each catalyst bed was never higher than 4 K. Furthermore, the difference between the mean temperatures of the three reactor sections did not exceed 4 K. We therefore decided to consider our reactor in the model calculations as an isothermal GSSTFR. The mean temperature $\bar{T}$ is calculated according to

$$\bar{T} = \frac{1}{3} \sum_{i=1}^{3} \frac{T_{upper,i} + T_{lower,i}}{2} \qquad (5)$$

where $T_{upper,i}$ and $T_{lower,i}$ are the true values of the temperatures of the gas at the upper and lower reactor ends, respectively, of reactor section $i$. We neglected possible radial temperature gradients in the catalyst bed and took $\bar{T}$ to be the temperature for the calculation of the predicted conversion in a isothermal GSSTFR. The error introduced due to this approach is small in comparison to that caused by taking the average reactor temperature in the three reactor sections.

Table 5. Typical temperature readouts. Experiment No. 34

| Location of the thermocouple (see Fig. 1) | Temperature measured (K) |
|---|---|
| Upper storage tank | 293.0 |
| Solids preheater | |
| Top[†] | 509.0 |
| Bottom | 510.0 |
| Gas outlet[†] | 473.0 |
| *First reactor section:* | |
| Top inside[†] | 508.6 |
| Wall | 508.3 |
| Bottom inside | 509.4 |
| Wall | 509.0 |
| First cooler, outside[†] | 509.0 |
| *Second reactor section:* | |
| Top inside[†] | 511.0 |
| Wall | 510.6 |
| Bottom inside | 511.8 |
| Wall | 511.3 |
| Second cooler, outside[†] | 507.0 |
| *Third reactor section:* | |
| Top inside[†] | 504.6 |
| Wall | 504.0 |
| Bottom, inside | 508.0 |
| Wall | 506.9 |
| Gas preheater[†] | 510.0 |
| Solids cooler | 373.0 |
| Lower storage tank | 293.0 |

[†]Control temperatures. These temperatures are used to adjust the rate of heat supply in the heating elements.

As our entire installation was built for operation at much higher pressures and temperatures—in our case for $NH_3$ synthesis—the wall thicknesses, etc. are relatively great. The heat capacity of the installation in comparison to the heat produced by the reaction is very large, so it can be expected that our reactor sections operate under near isothermal conditions. A large-scale industrial GSSTFR, of course, would operate adiabatically, as has been argued in our previous paper (Westerterp and Kuczynski, 1987).

In Fig. 6 the conversions of CO as determined for experiments without solids flow are compared with those calculated for an isothermal PFR and for the kinetics given in the paper by Kuczynski *et al.* (1986a). The agreement is reasonable.

The comparison of the experimental CO conversions for the experiments with flow of solids and the values predicted by our theoretical model of the GSSTF reactor (Westerterp and Kuczynski, 1987) is illustrated by Fig. 7. Despite a rather large spread in the data points, no systematic deviations can be observed. Further, we see that conversions higher than the thermodynamic equilibrium conversion in a solids-stream-free system are obtained in the GSSTFR.

Figure 8 shows a comparison between the experimental and the theoretically predicted reactor capacities in the case of *complete conversion of the reactants*. Reasonable agreement can be observed; the deviations can, among other things, be ascribed to inaccuracies in the kinetic correlation used in the model computations.

## 5. CONCLUSIONS

We can conclude from our experimental results that complete conversion is attainable in single-pass operation of a countercurrent GSSTFR fed with an adsorbent which selectively adsorbs only the product. An increase in the flow of the solids results in a decrease of the partial pressure of the product in the gas phase, so that conversion rates approaching the initial reaction rate can be maintained over the whole reactor length.
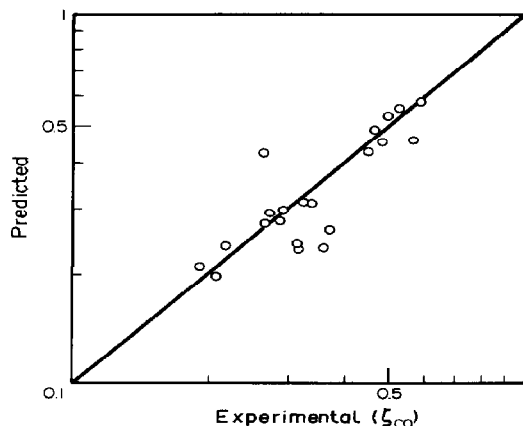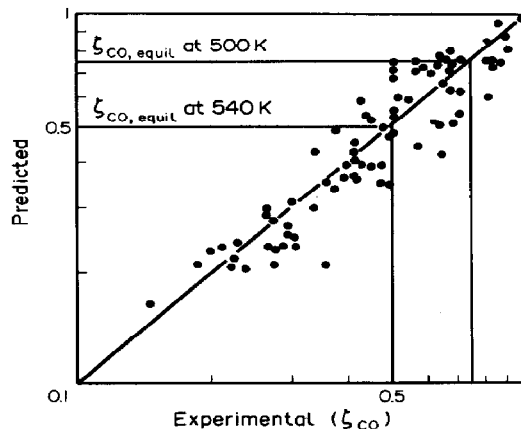


Fig. 7. Comparison of the experimentally determined conversions and those predicted by our model (Westerterp and Kuczynski, 1987) in the case of an open reactor outlet.
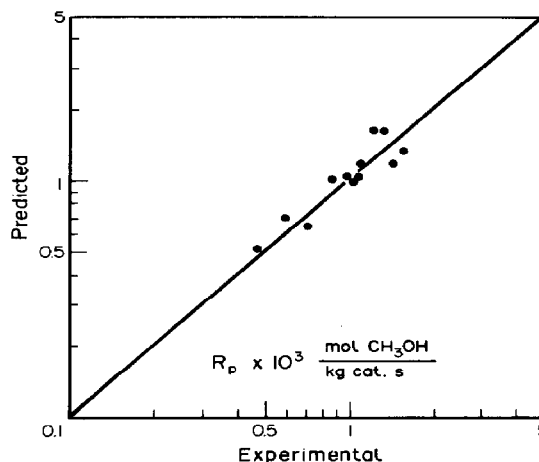


Fig. 8. Comparison of the measured reactor capacities and those predicted by our model (Westerterp and Kuczynski 1987) in the case of a closed reactor outlet.

Also operation at incomplete conversion is possible, in which the non-converted reactants together with non-adsorbed product leave the reactor at the top. The granulated silica–alumina cracking catalyst is selective for the adsorption of methanol.

The experimental results agree well with the predictions obtained with the theoretical model presented previously. The spread in the data points is, in addition to experimental errors, ascribed to unpredictable effects such as the influence of various undesired gas components on the properties and activity of the catalyst.

Fig. 6. Comparison of the measured CO conversions in the GSSTFR without solids flow with those predicted with the model.

## NOTATION

| | |
|---|---|
| $A, B$ | parameters in eq. (A3) |
| $c_{p,g}$ | heat capacity of gas, $J kg^{-1} K^{-1}$ |
| $d_t$ | diameter of the thermocouple, m |
| $D$ | parameter in eq. (A2) |
| $L$ | length of the thermocouple, m |
| $m$ | parameter in eqs (A2) and (A4), $m^{-1}$ |
| $m(T)$ | distribution factor (see text), |

$$\left(\frac{mol\ CH_3OH}{m^3\ solid}\right)\Bigg/\left(\frac{mol\ CH_3OH}{m^3\ gas}\right)$$

| | |
|---|---|
| $m_{cat}$ | mass of catalyst, kg |
| $p$ | total pressure, Pa |
| $Pr_g$ | Prandtl number $= (c_{p,g}\mu_g)/\lambda_g$ |
| $R$ | gas constant $= 8.3144,\ J\ mol^{-1} K^{-1}$ |
| $Re$ | Reynolds number $= (\rho_g u_g d_t)/\mu_g$ |
| $R_P$ | reaction rate of methanol formation, mol $CH_3OH\ (kg\ cat\ s)^{-1}$ |
| $Nu$ | Nusselt number $= \alpha d_t/\lambda_g$ |
| $T$ | absolute temperature, K |
| $\bar{T}$ | mean temperature [see eq. (5)], K |
| $T_G$ | temperature of gas, K |
| $T_L$ | temperature of the reactor wall, K |
| $T_o$ | temperature measured in the reactor axis, K |
| $T_R$ | reference temperature (542.2 K), K |
| $u_g$ | approach velocity of the gas, $m\ s^{-1}$ |
| $x$ | axial coordinate, m |
| $y_{CO,in}$ | mole fraction of CO in the feed gas |

*Greek letters*

| | |
|---|---|
| $\alpha^*$ | ratio of methanol flow rates carried over and produced, respectively |
| $\alpha$ | convective heat-transfer coefficient, $W\ m^{-2} K^{-1}$ |
| $\alpha_E$ | convective heat-transfer coefficient for the end face of the thermocouple, $W\ m^{-2} K^{-1}$ |
| $\phi_{in}$ | feed gas flow, $mol\ s^{-1}$ |
| $\phi_s$ | solids flow, $kg\ s^{-1}$ |
| $\delta$ | catalyst activity factor [see text below eq. (4)] |
| $\lambda$ | thermal conductivity of the thermocouple material, $W\ m^{-1} K^{-1}$ |
| $\lambda_g$ | thermal conductivity of the gas, $W\ m^{-1} K^{-1}$ |
| $\rho_g$ | density of the gas, $kg\ m^{-3}$ |
| $\rho_s$ | particle density of the adsorbent, $kg\ m^{-3}$ |
| $\mu_g$ | dynamic viscosity of the gas, $Pa\ s$ |

## REFERENCES

Herman, R. G., Klier, K., Simmons, G. W., Finn, B. P., Bulko, J. B. and Kobylinski, T. P., 1979, Catalytic synthesis of methanol from $CO/H_2$. I. *J. Catal.* **56**, 407–429.
Kuczynski, M., Browne, W. I., Fontein, H. J. and Westerterp, K. R., 1986a, Reaction kinetics for the synthesis of methanol from CO and $H_2$ on a copper catalyst. *Chem. Engng Proc.* (in press).
Kuczynski, M., van Ooteghem, A. and Westerterp, K. R., 1986b, Methanol adsorption by amorphous silica alumina in the critical temperature range. *Colloid Polymer Sci.* **264**, 362–367.
Noordergraaf, I. W., Roes, A. W. M. and van Swaaij, W. P. M., 1980a, Experimental study on the behaviour of a gas–solid countercurrent zig-zag contactor at trickle flow. *Proc. 2nd Powder Eur. Conf.*, Wiesbaden, F.R.G.
Noordergraaf, I. W., Roes, A. W. M. and van Swaaij, W. P. M.,

1980b, Axial mixing and mass transfer in a zig-zag contactor. *Proc. 3rd Conf. Fluidization*, Henniker, U.S.A., pp. 341–348.
Noordergraaf, I. W., Verver, A. B. and van Swaaij, W. P. M., 1980c, Gas-Feststoff Rieselströmung und Austauschprozesse in einem Zickzack-Kontaktor. *TIZ-Fachberichte Rohstoff-Engineering* **104**, 534–536.
Perry, J. H. and Chilton, C. H., 1979, *Chemical Engineer's Handbook*, 5th edn. McGraw-Hill, New York.
Roes, A. W. M., 1978, The behaviour of a gas–solid packed column at trickle flow. Thesis, Twente University of Technology, The Netherlands.
Roes, A. W. M. and van Swaaij, W. P. M., 1979a, Hydrodynamic behaviour of a gas–solid countercurrent packed column at trickle flow. *Chem. Engng J.* **17**, 81–89.
Roes, A. W. M. and van Swaaij, W. P. M., 1979b, Axial dispersion of gas and solid phases in a gas–solid packed column at trickle flow. *Chem. Engng J.* **18**, 13–28.
Roes, A. W. M. and van Swaaij, W. P. M., 1979c, Mass transfer in a gas–solid packed column at trickle flow. *Chem. Engng J.* **18**, 29–37.
Verver, A. B., 1984, The catalytic oxidation of hydrogen sulphide to sulphur in a gas–solid trickle flow reactor. Thesis, Twente University of Technology, The Netherlands.
Westerterp, K. R. and Kuczynski, M., 1986, Retrofit methanol plants with this converter system. *Hydrocarb. Process.* **11**, 80–83.
Westerterp, K. R. and Kuczynski, M., 1987, A model for a countercurrent gas–solid–solid trickle flow reactor for equilibrium reactions. The methanol synthesis. *Chem. Engng Sci.* **42**, 1871–1885.

## APPENDIX

In the experiments both the temperature $T_L$ of the reactor wall and $T_o$ in the reactor axis were measured (see Fig. A1). We assume the temperature $T_G$ of the gas surrounding the thermocouple to be uniform.

The differential steady-state heat balance for the thermocouple is

$$\frac{d^2 T}{dx^2} = \frac{4\alpha}{\lambda d_t}(T_G - T) \qquad (A1)$$

with $\alpha$ the convective heat-transfer coefficient assumed to be constant along the thermocouple, $\lambda$ the heat conductance of the thermocouple material and $d_t$ the thermocouple diameter. Taking the following boundary conditions:

$$x = 0, \quad \alpha_E(T_G - T_o) = -\lambda \frac{dT}{dx}$$

where $\alpha_E$ is the convective heat-transfer coefficient for the end face of the thermocouple and
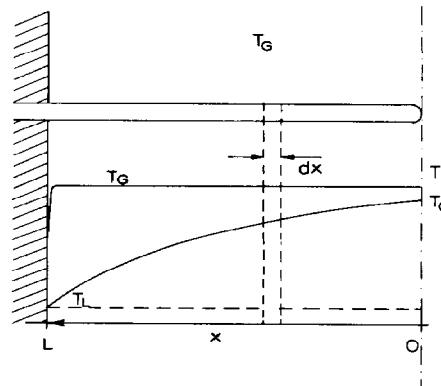
$$x = L, \quad T = T_L.$$



Fig. A1. Temperature profile in the thermocouple.

For these boundary conditions the differential equation can be easily solved. The temperature $T_o$ of the tip of the thermocouple is thus found to be given by

$$\frac{T_G - T_L}{T_o - T_L} = \cosh(mL) + D\sinh(mL) \qquad \text{(A2)}$$

with $m = \sqrt{\dfrac{4\alpha}{\lambda d_t}}$ and $D = \dfrac{\alpha_E}{\lambda m}$. Assuming $\alpha_E \approx \alpha$, the solution becomes

$$\frac{T_G - T_L}{T_o - T_L} = \left[\frac{4B}{(2B+A)e^{2AB} + (2B-A)e^{-2AB}}\right]^{-1} \qquad \text{(A3)}$$

with $A = \sqrt{\dfrac{\alpha L}{\lambda}}$ and $B = \sqrt{\dfrac{L}{d_t}}$.

If the heat transfer through the end face of the thermocouple can be neglected, then for $x = 0$ $dT/dx = 0$ holds and the solution is

$$\frac{T_G - T_L}{T_o - T_L} = \cosh(mL). \qquad \text{(A4)}$$

For the calculation of $\alpha$ we use the correlation (Perry and Chilton, 1979)

$$Nu = 0.989 \, Re^{1/3} \, Pr^{0.33}$$

where

$$Nu = \frac{\alpha d_t}{\lambda_g}, \quad Re = \frac{u_g d_t \rho_g}{\mu_g} \quad \text{and} \quad Pr_g = \frac{c_{p,g}\mu_g}{\lambda_g}$$

in which $c_{p,g}$ represents the heat capacity and $\lambda_g$ the thermal conductivity of the gas.

Under the conditions of our experiments ($\lambda = 22.5$ $W\,m^{-1}\,K^{-1}$, $d_t = 1.6 \times 10^{-3}$ m, $L = 12.5 \times 10^{-3}$ m and $Pr \approx 0.7$), the heat transfer through the end face of the thermocouple cannot be neglected. The tip area is 3% of the total external area of the thermocouple, so we prefer the use of eq. (A3). The ratio $(T_G - T_L)/(T_o - T_L)$ lies between 1.6 and 3.5, or $T_G - T_o$ is 0.6–2.5 times the measured temperature difference $T_o - T_L$.